JYX JYVÄSKYLÄN YLIOPISTO UNIVERSITY OF JYVÄSKYLÄ

This is a self-archived version of an original article. This version may differ from the original in pagination and typographic details.

Author(s): Stan, Adrian; Dahlen, N.E.; van Leeuwen, Robert

Title: Levels of self-consistency in the GW approximation

Year: 2009

Version: Published version

Copyright: © 2009 American Institute of Physics.

Rights: In Copyright

Rights url: http://rightsstatements.org/page/InC/1.0/?language=en

Please cite the original version:

Stan, A., Dahlen, N.E., & van Leeuwen, R. (2009). Levels of self-consistency in the GW approximation. Journal of chemical physics, (130), 114105. https://doi.org/10.1063/1.3089567

The Journal of Chemical Physics

Levels of self-consistency in the GW approximation

Cite as: J. Chem. Phys. **130**, 114105 (2009); https://doi.org/10.1063/1.3089567
Submitted: 04 December 2008 . Accepted: 06 February 2009 . Published Online: 19 March 2009

Adrian Stan, Nils Erik Dahlen, and Robert van Leeuwen

View Online Export Citation

ARTICLES YOU MAY BE INTERESTED IN

Self-consistent solution of the Dyson equation for atoms and molecules within a conserving approximation
The Journal of Chemical Physics **122**, 164102 (2005); https://doi.org/10.1063/1.1884965

Self-consistent second-order Green's function perturbation theory for periodic systems
The Journal of Chemical Physics **144**, 054106 (2016); https://doi.org/10.1063/1.4940900

Time propagation of the Kadanoff–Baym equations for inhomogeneous systems
The Journal of Chemical Physics **130**, 224101 (2009); https://doi.org/10.1063/1.3127247

© 2009 American Institute of Physics.

Levels of self-consistency in the *GW* approximation

Adrian Stan,[1,2,a)] Nils Erik Dahlen,[2] and Robert van Leeuwen[1]
[1]*Department of Physics, Nanoscience Center, University of Jyväskylä, Jyväskylä FIN 40014, Finland*
[2]*Rijksuniversiteit Groningen, Zernike Institute for Advanced Materials, Nijenborgh 4, 9747AG Groningen, The Netherlands*
[3]*European Theoretical Spectroscopy Facility (ETSF), Jyväskylä FIN 40014, Finland*

(Received 4 December 2008; accepted 6 February 2009; published online 19 March 2009)

We perform *GW* calculations on atoms and diatomic molecules at different levels of self-consistency and investigate the effects of self-consistency on total energies, ionization potentials, and particle number conservation. We further propose a partially self-consistent *GW* scheme in which we keep the correlation part of the self-energy fixed within the self-consistency cycle. This approximation is compared to the fully self-consistent *GW* results and to the GW_0 and the G_0W_0 approximations. Total energies, ionization potentials, and two-electron removal energies obtained with our partially self-consistent *GW* approximation are in excellent agreement with fully self-consistent *GW* results while requiring only a fraction of the computational effort. We also find that self-consistent and partially self-consistent schemes provide ionization energies of similar quality as the G_0W_0 values but yield better total energies and energy differences. © *2009 American Institute of Physics*. [DOI: 10.1063/1.3089567]

I. INTRODUCTION

Green function methods[1,2] have been very successful in the description of various properties of many-electron systems, ranging from atoms and molecules to solids.[3,4] Within the Green function approach, these properties are completely determined by the self-energy operator Σ, which incorporates all the effects of exchange and correlation in a many-particle system.[1] One of the most widely used approximations to the self-energy is the *GW* approximation (GWA).[5] In the GWA, the self-energy operator has the simple form $\Sigma = -GW$, where G is the Green function that describes the propagation of particles and holes in the system and W is the dynamically screened interaction. This quantity describes how the bare interaction v between electrons is modified due to the presence of the other electrons and appears as a renormalized interaction in terms of Feynman diagrams. In extended systems the screened interaction is much weaker than the bare interaction, and therefore it is much more natural to expand the self-energy in terms of the screened interaction than in terms of the bare interaction. The lowest order in this expansion[5] is the GWA.

Calculations within the GWA are usually done in two steps. First, a density functional theory[6] (DFT) calculation is performed and the DFT orbitals and eigenvalues are used to construct a first guess G_0 for the Green function and a first guess W_0 for the screened interaction. In a second step, the self-energy $\Sigma = -G_0W_0$ is constructed and the Dyson equation is solved for the Green function. In principle, this new Green function should be used to calculate a new self-energy and this process should be iterated to self-consistency.[5] However, one usually stops after the first iteration. The corresponding approximation for the Green function is known as the G_0W_0 approximation and has become one of the most accurate methods for the calculation of spectral properties and band gaps of solids.[3,4] One reason for not going beyond the first iteration of the G_0W_0 method is the large computational cost involved. There are further indications that a full self-consistent solution would worsen the spectral properties as a consequence of a cancellation between dressing of Green functions and vertex corrections.[7] This was investigated for the electron gas[8] and the Hubbard model.[9] However, this problem has not been investigated in detail for real systems mainly due to the computational cost involved.

The G_0W_0 approximation has, however, two unsatisfactory aspects. The first aspect is related to the satisfaction of conservation laws. Baym[10] showed that the self-energy expressions that can be obtained as a functional derivative of a functional $\Phi[G]$ of the Green function, i.e., $\Sigma = \delta\Phi/\delta G$, have the important property that they lead to conserving many-body approximations. These approximations obey basic conservation laws, like the ones for particle number, momentum, angular momentum, and energy. The GWA is one of these conserving schemes.[11–13] However, the Φ-derivable approximations are only conserving when the Dyson equation for the Green function is solved fully self-consistently. A lack of full self-consistency will generally result in a violation of the conservation laws. For this reason the use of conserving approximations, such as *GW*, is crucial in obtaining a correct description of transport phenomena within a nonequilibrium Green function approach.[14–18] Since it is one of our research goals to study quantum transport, it will be necessary to consider the fully self-consistent *GW* (SC-*GW*) approximation.[8,19–24]

A second unsatisfactory aspect of non-self-consistent schemes, such as G_0W_0, is that the values of the observables depend on the way they are calculated. For instance, the total energy can be calculated in different ways from the Green

[a)]Electronic mail: adrian.stan@jyu.fi.

 © 2009 American Institute of Physics

function and the self-energy: using the Galitskii–Migdal formula,[25] a coupling constant integration,[22] a Luttinger–Ward expression,[13,26–28] or various other expressions. For non-self-consistent calculations all these expressions lead to different results and therefore to ambiguity in the value of the energy. It was, however, demonstrated in the work of Baym[10] that self-consistent Φ-derivable approximations are not only conserving but also have the property that all the various ways in which the observables are calculated provide the same result. This is another motivation for considering fully self-consistent many-body schemes.

We can therefore conclude that self-consistency is important to obtain conserving and unambiguous results. However, the large computational cost of self-consistent schemes makes them unattractive for the calculation of the properties of large and extended systems. In order to lower the computational effort it is possible to use partial self-consistency which may result in a less severe violation of conservation laws. One can, for instance, keep the screened interaction fixed during iteration of the Dyson equation. This leads to a scheme that can be shown to still conserve the particle number and that has been tested on the electron gas.[23,29] Another approach in which the self-consistency is constrained is the so-called quasiparticle self-consistent *GW* (QSGW) method.[30–33] In this approach a frequency independent self-energy of *GW* form is constructed and used to solve a quasiparticle equation from which the Green function and the screened interaction are constructed iteratively. Due to the Hermitian nature of the self-energy the method leads to an orthonormal set of quasiparticle states and thereby restricts the form of the Green function and the screened interaction. This method has been successful in improving the G_0W_0 band gaps and band widths for a large range of solids.[32] One could further consider similar other approximations within a quasiparticle framework.[34] Such approximations have been shown to improve the band structure when local density approximation (LDA) is a poor starting point. These methods are, however, not Φ-derivable and are in general not conserving. Extending methods based on quasiparticle equations to the time-dependent case is not as straightforward as for the SC-*GW*, GW_0, and G_0W_0 methods, which are instead based on an equation of motion for the Green function. For the same reason the computational schemes used in this paper (which aims at an extension to the time-dependent case) would need to be modified in order to do QSGW calculations. We therefore did not consider the QSGW method in this work. However, we propose another partially self-consistent scheme which is computationally cheaper than the GW_0 method. In this approximation the correlation part of the self-energy is fixed during the iteration cycle while only the Hartree and exchange parts are updated self-consistently. In this paper we investigate this approximation and other *GW* schemes at different levels of self-consistency and test them on atoms and diatomic molecules. We also present in more detail the computational method behind the SCGW calculations that we described briefly in an earlier letter.[35] The paper is divided as follows: In Sec. II we briefly present the general formalism and in Sec. III we describe in detail the GWA at different levels of self-consistency. We then present in Sec. IV the details of our computational procedure. Finally, in Sec. V, we will discuss the results obtained with the GWA at different levels of self-consistency for atoms and some diatomic molecules. These systems are well suited in testing the *GW* at different levels of self-consistency, but we are ultimately interested in applications in quantum transport theory for molecules attached to macroscopic leads. In such applications the long range screening effects, as incorporated in the GWA, are important. The investigations in this paper are a first step in this direction and aim to get further insight into various aspects of the GWA that are relevant in quantum transport theory.

II. GENERAL FORMALISM

We study finite many-particle systems using the Matsubara formalism[1,36] which can easily be extended to a nonequilibrium version of the theory.[37–39] We consider a many-body system in thermal equilibrium at a temperature T and chemical potential μ, and with the Hamiltonian (in second quantization[1])

$$\hat{H} = \int d\mathbf{x}\hat{\psi}^\dagger(\mathbf{x})h(\mathbf{r})\hat{\psi}(\mathbf{x}) + \frac{1}{2}\int\int d\mathbf{x}_1 d\mathbf{x}_2 \hat{\psi}^\dagger(\mathbf{x}_1)\hat{\psi}^\dagger(\mathbf{x}_2)v(\mathbf{r}_1,\mathbf{r}_2)\hat{\psi}(\mathbf{x}_2)\hat{\psi}(\mathbf{x}_1). \tag{1}$$

Here $\mathbf{x}=(\mathbf{r},\sigma)$ denotes the space and spin coordinates. The two-body interaction v is taken to be of Coulombic form $v(\mathbf{r}_1,\mathbf{r}_2)=1/|\mathbf{r}_1-\mathbf{r}_2|$. We use atomic units $\hbar=m=e=1$ throughout this paper. The single particle part of the Hamiltonian $h(\mathbf{r})$ has the explicit form

$$h(\mathbf{r}) = -\tfrac{1}{2}\nabla^2 + w(\mathbf{r}) - \mu, \tag{2}$$

where $w(\mathbf{r})$ is the external potential and where we absorbed the chemical potential μ into h. The equilibrium expectation value of an operator $\hat{O}$ in the grand canonical ensemble is then given by

$$\langle\hat{O}\rangle = \mathrm{Tr}\{\hat{\rho}\hat{O}\}, \tag{3}$$

where $\hat{\rho}=e^{-\beta\hat{H}}/\mathrm{Tr}\, e^{-\beta\hat{H}}$ is the statistical operator, $\beta=1/k_BT$ the inverse temperature, and k_B the Boltzmann constant. The trace is taken over all states in Fock space.[1] The Green function is then defined as

$$G(\mathbf{x}\tau_1,\mathbf{x}'\tau_2) = -\theta(\tau_1-\tau_2)\langle\hat{\psi}_H(\mathbf{x}\tau_1)\hat{\psi}_H^\dagger(\mathbf{x}'\tau_2)\rangle + \theta(\tau_2-\tau_1)\langle\hat{\psi}_H^\dagger(\mathbf{x}'\tau_2)\hat{\psi}_H(\mathbf{x}\tau_1)\rangle, \tag{4}$$

where we define the Heisenberg form of the operators in this equation to be $\hat{O}_H=e^{\tau\hat{H}}\hat{O}e^{-\tau\hat{H}}$. Since the Hamiltonian is time-translation invariant, the equilibrium Green function only depends on the difference between the time coordinates: $G(\mathbf{x}\tau_1,\mathbf{x}'\tau_2)=G(\mathbf{x},\mathbf{x}';\tau_1-\tau_2)$. The Green function satisfies the equation of motion

$$[-\partial_\tau - h(\mathbf{r})]G(\mathbf{x},\mathbf{x}';\tau) = \delta(\tau)\delta(\mathbf{x}-\mathbf{x}') + \int_0^\beta d\tau_1 \int d\mathbf{x}_1 \times \Sigma[G](\mathbf{x},\mathbf{x}_1;\tau-\tau_1)G(\mathbf{x}_1,\mathbf{x}';\tau_1), \quad (5)$$

where the self-energy $\Sigma[G](\mathbf{x},\mathbf{x}';\tau)$ incorporates the many-body interactions of the system. The self-energy can be approximated with the usual diagrammatic methods.[1,2] Since $\Sigma[G]$ is a functional of the Green function Eq. (5) must be solved self-consistently. The self-energy is usually split into a Hartree part and an exchange-correlation part according to

$$\Sigma[G](\mathbf{x}_1,\mathbf{x}_2;\tau) = \delta(\tau)\delta(\mathbf{x}_1-\mathbf{x}_2)v_H(\mathbf{r}_1) + \Sigma_{\mathrm{xc}}[G](\mathbf{x}_1,\mathbf{x}_2;\tau), \quad (6)$$

where the Hartree potential is defined as the potential due to the electron charge by

$$v_H(\mathbf{r}) = \int d\mathbf{x}' n(\mathbf{x}')v(\mathbf{r},\mathbf{r}'), \quad (7)$$

where we introduced the electron density

$$n(\mathbf{x}) = \lim_{\eta\to 0} G(\mathbf{x},\mathbf{x};-\eta). \quad (8)$$

The main task is now to find an approximation for this exchange-correlation part Σ_{xc} of the self-energy and to solve Eq. (5). We convert Eq. (5) to integral form[40]

$$G(\mathbf{x}_1,\mathbf{x}_2;\tau) = G_0(\mathbf{x}_1,\mathbf{x}_2;\tau) + \int_0^\beta d\tau_1 d\tau_2 \int d\mathbf{x}_3 d\mathbf{x}_4 G_0(\mathbf{x}_1,\mathbf{x}_3;\tau-\tau_1) \times (\Sigma[G](\mathbf{x}_3,\mathbf{x}_4;\tau_1-\tau_2) - \delta(\tau_1-\tau_2)\Sigma_0(\mathbf{x}_3,\mathbf{x}_4))G(\mathbf{x}_4,\mathbf{x}_2;\tau_2). \quad (9)$$

Here we introduced a static reference self-energy Σ_0 and a reference Green function G_0 which is defined by the equation

$$[-\partial_\tau - h(\mathbf{r})]G_0(\mathbf{x},\mathbf{x}';\tau) = \delta(\tau)\delta(\mathbf{x}-\mathbf{x}') + \int d\mathbf{x}_1 \Sigma_0(\mathbf{x},\mathbf{x}_1)G_0(\mathbf{x}_1,\mathbf{x}';\tau). \quad (10)$$

In practice we solve first Eq. (10) for G_0 and then we solve Eq. (9) for G. It is clear from Eq. (5) that a fully self-consistent solution of Eq. (9) does not depend on the reference Green function G_0. In this work we choose for Σ_0 a Hartree–Fock (HF) or a density functional self-energy. In the first case $\Sigma_0 = v_H[G_0] + \Sigma_x[G_0]$, consisting of Hartree and exchange parts, whereas in the second case $\Sigma_0 = \delta(\mathbf{x}-\mathbf{x}')v_{H\mathrm{xc}}[G_0](\mathbf{x})$, where $v_{H\mathrm{xc}}(\mathbf{x})$ is the sum of the Hartree and the exchange-correlation potential.[6]

From the Green function several observables can be calculated. To calculate the total energy $E = T + V_{ne} + U_0 + U_{\mathrm{xc}}$ we use the fact that the exchange-correlation part U_{xc} of the interaction energy is given by[1,2]

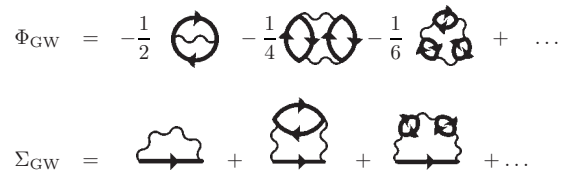

FIG. 1. The GW self-energy Σ is the functional derivative of a functional $\Phi[G]$.

$$U_{\mathrm{xc}} = \frac{1}{2}\int_0^\beta d\tau \int d\mathbf{x}_1 \int d\mathbf{x}_2 \Sigma_{\mathrm{xc}}(\mathbf{x}_1,\mathbf{x}_2;-\tau)G(\mathbf{x}_2,\mathbf{x}_1;\tau). \quad (11)$$

The kinetic energy T, the nuclear-electron attraction energy V_{ne}, and the Hartree energy $U_0 = 1/2\int d\mathbf{r}d\mathbf{r}' n(\mathbf{r})v(\mathbf{r},\mathbf{r}')n(\mathbf{r}')$ can all be calculated directly from the Green function. To calculate the ionization potentials from the Green function we used the extended Koopmans theorem,[41–45] a short derivation of which is given in Appendix B.

III. THE *GW* APPROXIMATION AT DIFFERENT LEVELS OF SELF-CONSISTENCY

A. Fully self-consistent *GW*

Within the GWA the exchange-correlation part of the self-energy has the explicit form[5,46,47]

$$\Sigma_{\mathrm{xc}}(\mathbf{x}_1,\mathbf{x}_2;\tau) = -G(\mathbf{x}_1,\mathbf{x}_2;\tau)W(\mathbf{x}_1,\mathbf{x}_2;\tau), \quad (12)$$

in which W is a dynamically screened interaction corresponding to an infinite summation of bubble diagrams (see Fig. 1). From this figure we see that this self-energy is given as a functional derivative of a functional $\Phi[G]$ with respect to G and hence represents a conserving approximation.[10] From the diagrammatic structure we see that the screened potential W satisfies the equation

$$W(\mathbf{x}_1,\mathbf{x}_2;\tau) = v(\mathbf{r}_1,\mathbf{r}_2)\delta(\tau) + \int d\mathbf{x}_3 d\mathbf{x}_4 \int_0^\beta d\tau' v(\mathbf{r}_1,\mathbf{r}_3) \times P(\mathbf{x}_3,\mathbf{x}_4;\tau-\tau')W(\mathbf{x}_4,\mathbf{x}_2;\tau'), \quad (13)$$

where v is the bare Coulomb interaction and P is the irreducible polarization,

$$P(\mathbf{x}_1,\mathbf{x}_2;\tau) = G(\mathbf{x}_1,\mathbf{x}_2;\tau)G(\mathbf{x}_2,\mathbf{x}_1;-\tau). \quad (14)$$

The problem is now completely defined. Equations (13) and (14) need to be solved self-consistently together with Eqs. (12), (6), and (9).

B. The G_0W_0 and GW_0 approximations

The G_0W_0 approximation, as mentioned before, is obtained from a single iteration of the Dyson equation (9), starting from a refence Green function G_0. For this approximation the self-energy is given as $\Sigma_{\mathrm{xc}}[G_0] = -G_0W_0$ where W_0 is calculated by inserting G_0 into Eq. (14) and solving Eq. (13) with this irreducible polarization. The Dyson equation (9) is then solved with this self-energy to obtain an improved Green function G from which spectral properties are calculated. In principle one should insert this Green func-

tion into the self-energy and solve the Dyson equation again for a new Green function. This procedure should be continued until self-consistency is achieved but this is rarely done in practice for the reasons mentioned in the Introduction.

We further consider a partially self-consistent scheme in which we write the self-energy as $\Sigma_{xc}[G,G_0]=-GW_0$, where the Green function G is determined fully self-consistently by repeated solution of the Dyson equation and where W_0 is calculated from G_0 in the same way as for the G_0W_0 approximation. This reduces the computational cost considerably as it avoids the self-consistent calculation of the screened interaction W. The corresponding approximation is known as the GW_0 approximation.[29,48] This approximation was shown to be number conserving by Holm and von Barth[49] for the case of homogeneous systems. More precisely they derived that the GW_0 approximation satisfies the Hugenholtz–van Hove theorem[50] for the homogeneous electron gas. However, one can readily derive the number conserving property for the inhomogeneous and time-dependent case. This requires nonequilibrium Green functions in the proof, but this extension is straightforward.[51] If we regard W_0 as a given potential (albeit nonlocal in space and time), it is clear that $\Sigma=\delta\Phi/\delta G$ for $\Phi[G,W_0]=-1/2\ \mathrm{tr}\ GGW_0$, where the trace denotes integration over space-time variables. Since this Φ is invariant under gauge transformations (the phases cancel at each vertex of Φ), we can follow the proof of Baym[10] and derive that GW_0 is particle conserving. However, for time-dependent and inhomogeneous systems W_0 is not invariant under spatial and time translations, unlike the bare interaction v that usually appears in the functional $\Phi[G]$. Therefore the GW_0 approximation will not be momentum or energy conserving.

C. The GW_{fc} approximation

The most time-consuming part of the GW_0 calculation is the evaluation of the correlation part of the self-energy which is nonlocal in time. We therefore propose another partial self-consistent scheme in which we only evaluate the time-local Hartree and exchange parts of the self-energy in a self-consistent manner. We therefore split the self-energy as follows:

$$\Sigma[G,G_0]=\Sigma^{\mathrm{HF}}[G]+\Sigma_c[G_0]. \tag{15}$$

The first term in this equation represents the HF part of the self-energy,

$$\Sigma^{\mathrm{HF}}[G]=v_H[G]+\Sigma_x[G], \tag{16}$$

which consists of a Hartree part and an exchange part $\Sigma_x[G]=-Gv$. The last term in Eq. (15) represents the correlation part of the self-energy and has the explicit form

$$\Sigma_c[G_0]=-G_0(W_0-v), \tag{17}$$

where W_0 is calculated from G_0 in the same way as for the G_0W_0 approximation. The approximation for the self-energy of Eq. (15) will be denoted as the GW_{fc} approximation (where fc stands for fixed correlation). This approximation is not conserving but, as we will see later, nevertheless produces observables in very close agreement with those obtained from a fully SC-GW calculation.

IV. COMPUTATIONAL METHOD

A. Numerical solution of the Dyson equation

In the following, we will describe the computational methods that we employed for calculating the Green function and the screened interaction W. We consider the case of spin-unpolarized systems where the Green function has the form

$$G(\mathbf{x},\mathbf{x}';\tau)=\delta_{\sigma\sigma'}G(\mathbf{r},\mathbf{r}';\tau). \tag{18}$$

The calculations are carried out using a set of basis functions such that the spin-independent part of the Green function is expressed as

$$G(\mathbf{r},\mathbf{r}';\tau)=\sum_{ij}G_{ij}(\tau)\phi_i(\mathbf{r})\phi_j^*(\mathbf{r}'). \tag{19}$$

The basis functions ϕ_i are represented as linear combinations of Slater functions $\psi_i(\mathbf{r})=r^{n_i-1}e^{-\lambda_i r}Y_{l_i}^{m_i}(\Omega)$ which are centered on the different nuclei and are characterized by quantum numbers (n_i,l_i,m_i) and an exponent λ_i. In these expressions and $Y_{l_i}^{m_i}(\Omega)$ are the usual spherical harmonics. The molecular orbitals ϕ_i and eigenvalues ϵ_i are obtained from a HF or DFT Kohn–Sham calculation in this basis. The particle number N is determined by the chemical potential. Since we consider closed shell systems we have $N/2$ doubly occupied HF or Kohn–Sham levels ϵ_i (some of which may be degenerate). We therefore choose μ such that $e_i=\epsilon_i-\mu<0$ for $i\leqslant N/2$ and $e_i>0$ for $i>N/2$. In the zero-temperature limit (we used $\beta=100$) the observables are insensitive to the value of μ, provided $\epsilon_{N/2}<\mu<\epsilon_{N/2+1}$. The reference Green function G_0 corresponding to the Hamiltonian $h_0+\Sigma_0$ (either HF or DFT) is diagonal in the basis $\{\phi_i\}$, i.e., in matrix form we have $G_{ij,0}(\tau)=\delta_{ij}G_{i,0}(\tau)$, where

$$G_{i,0}(\tau)=\theta(\tau)(n(e_i)-1)e^{-e_i\tau}+\theta(-\tau)n(e_i)e^{-e_i\tau}, \tag{20}$$

and $n(e_j)=(e^{\beta e_j}+1)^{-1}$ is the Fermi–Dirac distribution. The Dyson equation of Eq. (9) in basis representation has the form

$$G(\tau)=G_0(\tau)+\int_0^\beta d\tau'\int_0^\beta d\tau''G_0(\tau-\tau')\times\Sigma^c[G,G_0](\tau'-\tau'')G(\tau''), \tag{21}$$

where we denote

$$\Sigma^c[G,G_0](\tau)=\Sigma[G](\tau)-\delta(\tau)\Sigma_0[G_0], \tag{22}$$

and where all quantities are matrices. Since in the limit $\tau\to 0^-$, G yields the density matrix, it is convenient to solve the Dyson equation for negative τ, values. We therefore rewrite Eq. (21) as

$$G_{ij}(\tau)=\delta_{ij}G_{i,0}(\tau)+\sum_k\int_{-\beta}^0 d\tau_1\int_{-\beta}^0 d\tau_2 G_{i,0}(\tau-\tau_1)\times\Sigma_{ik}^c(\tau_1-\tau_2)G_{kj}(\tau_2), \tag{23}$$

with $\tau\in[-\beta,0]$ where we changed variables $\tau_1=\tau'-\beta$, $\tau_2=\tau''-\beta$ and used $G_0(\tau)=-G_0(\tau+\beta)$ with the same relation

for G.[40] We now discretize Eq. (23) using a trapezoidal rule on a time grid $(\tau^{(0)}=0,\tau^{(1)},\ldots,\tau^{(m)}=-\beta)$. Since the Green functions behave exponentially near the endpoints of the imaginary time interval $[-\beta,0]$, we used a uniform power mesh (UPM).[20] We briefly describe this mesh in Appendix B. The discretized version of Eq. (23) attains the form

$$\delta_{ij}G_{i,0}(\tau^{(p)})=\sum_{k,q}\left[\delta_{ik}\delta_{pq}-\frac{\Delta\tau^{(q)}}{2}Z_{ik}(\tau^{(p)},\tau^{(q)})\right]G_{kj}(\tau^{(q)}), \tag{24}$$

where we defined Z_{ik} as

$$Z_{ik}(\tau^{(p)},\tau^{(q)})=\int_{-\beta}^{0}d\tau G_{i,0}(\tau^{(p)}-\tau)\Sigma_{ik}^{c}(\tau-\tau^{(q)}). \tag{25}$$

The time steps are positive, where $\Delta\tau^{(q)}=\tau^{(q-1)}-\tau^{(q+1)}$ except at the endpoints where $\Delta\tau^{(0)}=\tau^{(0)}-\tau^{(1)}$ and $\Delta\tau^{(m)}=\tau^{(m-1)}-\tau^{(m)}$. For a fixed j, Eq. (24) represents a set of linear equations of the form

$$\sum_{Q_2}A_{Q_1,Q_2}\cdot x_{Q_2}^{(j)}=b_{Q_1}^{(j)}, \tag{26}$$

where

$$A_{Q_1,Q_2}=A_{(ip)(kq)}=\delta_{ik}\delta_{pq}-\frac{\Delta\tau^{(q)}}{2}Z_{ik}(\tau^{(p)},\tau^{(q)}),$$

and the vectors $x_{Q_2}^{(j)},b_{Q_1}^{(j)}$ are defined to be

$$x_{Q_2}^{(j)}=x_{kq}^{(j)}=G_{kj}(\tau^{(q)}),$$

$$b_{Q_1}^{(j)}=b_{ip}^{(j)}=\delta_{ij}G_{i,0}(\tau^{(p)}).$$

The self-energy Σ^c of Eq. (22) has the form

$$\Sigma_{ij}^{c}(\tau)=\Sigma_{c,ij}[G](\tau)+\delta(\tau)[\Sigma_{ij}^{\mathrm{HF}}[G(0^-)]-\Sigma_{ij}^{0}], \tag{27}$$

where Σ^{HF} is the HF part of the self-energy defined in Eq. (16) and $\Sigma_c[G]$ the remaining correlation part. The convolution integral (25) can therefore be simplified to

$$Z_{ik}(\tau^{(p)},\tau^{(q)})=G_{i,0}(\tau^{(p)}-\tau^{(q)})[\Sigma_{ik}^{\mathrm{HF}}[G(0^-)]-\Sigma_{ik}^{0}]+\int_{-\beta}^{0}d\tau G_{i,0}(\tau^{(p)}-\tau)\Sigma_{c,ik}(\tau-\tau^{(q)}). \tag{28}$$

When we specify the explicit form of Σ_c, the solution of the Dyson equation is reduced to a calculation of Eq. (28) together with the linear system of equations (26). What remains to be discussed is the calculation of the self-energy itself. This is discussed in the next section.

B. Numerical calculation of the screened potential: The product basis technique

To calculate the self-energy we need to solve the equation for the screened interaction. The screened interaction has a singular time-local part representing the bare interaction v. It is therefore convenient to subtract v from W and to treat its contribution to the self-energy explicitly (this is simply the exchange part of the self-energy). From the remaining time-nonlocal part of W, given by $\tilde{W}(\mathbf{r}_1,\mathbf{r}_2;\tau)=W(\mathbf{r}_1,\mathbf{r}_2;\tau)-\delta(\tau)v(\mathbf{r}_1,\mathbf{r}_2)$, we can calculate the correlation part of the self-energy,

$$\Sigma_c(\mathbf{r}_1,\mathbf{r}_2;\tau)=-G(\mathbf{r}_1,\mathbf{r}_2;\tau)\tilde{W}(\mathbf{r}_1,\mathbf{r}_2;\tau). \tag{29}$$

After this quantity has been calculated it can then simply be added to the HF part of the self-energy to obtain the full self-energy $\Sigma[G]$. The time-nonlocal part $\tilde{W}$ of the screened interaction satisfies the equation

$$\tilde{W}(\mathbf{r}_1,\mathbf{r}_2;\tau)=\int d\mathbf{r}_3d\mathbf{r}_4v(\mathbf{r}_1,\mathbf{r}_3)P(\mathbf{r}_3,\mathbf{r}_4;\tau)v(\mathbf{r}_4,\mathbf{r}_2)+\int_0^{\beta}d\tau'\int d\mathbf{r}_3d\mathbf{r}_4v(\mathbf{r}_1,\mathbf{r}_3)\times P(\mathbf{r}_3,\mathbf{r}_4;\tau-\tau')\tilde{W}(\mathbf{r}_4,\mathbf{r}_2;\tau'), \tag{30}$$

where

$$P(\mathbf{r}_1,\mathbf{r}_2;\tau)=2G(\mathbf{r}_1,\mathbf{r}_2;\tau)G(\mathbf{r}_2,\mathbf{r}_1;-\tau). \tag{31}$$

The factor of 2 in this expression results from spin integrations in the equation of W using the form of the Green function of Eq. (18). We now insert into Eq. (31) the basis set expansion for the Green function of Eq. (19) to obtain

$$P(\mathbf{r}_1,\mathbf{r}_2;\tau)=\sum_{ijkl}P_{ijkl}(\tau)\phi_i(\mathbf{r}_1)\phi_j^*(\mathbf{r}_2)\phi_k(\mathbf{r}_2)\phi_l^*(\mathbf{r}_1), \tag{32}$$

where $P_{ijkl}=2G_{ij}(\tau)G_{kl}(-\tau)$. By defining the two-electron integrals

$$\tilde{W}_{pqrs}(\tau)=\int d\mathbf{r}_1d\mathbf{r}_2\phi_p^*(\mathbf{r}_1)\phi_q^*(\mathbf{r}_2)\tilde{W}(\mathbf{r}_1,\mathbf{r}_2;\tau)\phi_r(\mathbf{r}_2)\phi_s(\mathbf{r}_1),$$

$$v_{pqrs}=\int d\mathbf{r}_1d\mathbf{r}_2\phi_p^*(\mathbf{r}_1)\phi_q^*(\mathbf{r}_2)v(\mathbf{r}_1,\mathbf{r}_2)\phi_r(\mathbf{r}_2)\phi_s(\mathbf{r}_1),$$

we transform Eq. (30) into the equation

$$\tilde{W}_{pqrs}(\tau)=\sum_{ijkl}v_{plis}P_{ijkl}(\tau)v_{jqrk}+\sum_{ijkl}\int_0^{\beta}d\tau'v_{plis}P_{ijkl}(\tau-\tau')\tilde{W}_{jqrk}(\tau'). \tag{33}$$

If we use the multi-indices $Q_1=(ps)$, $Q_2=(rq)$, $Q_3=(il)$, and $Q_4=(jk)$, then we can write this equation in a more convenient form as

$$\tilde{W}_{Q_1Q_2}(\tau)=\sum_{Q_3Q_4}v_{Q_1Q_3}P_{Q_3Q_4}(\tau)v_{Q_4Q_2}+\sum_{Q_3Q_4}\int_0^{\beta}d\tau'v_{Q_1Q_3}P_{Q_3Q_4}(\tau-\tau')\tilde{W}_{Q_4Q_2}(\tau'), \tag{34}$$

where we defined $v_{il,kj}=v_{ijkl}$ and similarly for $\tilde{W}$ and $P_{il,jk}=P_{ijkl}$. We have now obtained an equation which we can

solve with the same algorithm we used for the Dyson equation.

Note that in this case we effectively use a product basis $f_q(\mathbf{r})=\phi_i(\mathbf{r})\phi_j^*(\mathbf{r})$, where $q=(ij)$ is a multi-index. This product basis is nonorthogonal and its size is in general much larger than we need in practice due to linear dependencies. We thus follow a technique developed by Aryasetiawan and Gunnarsson[52] which allows to reduce significantly the size of the product basis $\{f_q(\mathbf{r})\}$ and the computational cost.

The overlap matrix S for the set of orbitals $f_q(\mathbf{r})$,

$$S_{qq'}=\langle f_q|f_{q'}\rangle, \tag{35}$$

is diagonalized by a unitary matrix U,

$$\sum_{q_1q_2} U^\dagger_{qq_1}\langle f_{q_1}|f_{q_2}\rangle U_{q_2q'}=\sigma_q\delta_{qq'}, \tag{36}$$

where the eigenvalues σ_q are positive since S is a positive definite matrix. We now define a new set of orthonormal orbitals g_q as

$$g_q(\mathbf{r})=\frac{1}{\sqrt{\sigma_q}}\sum_{q'} U_{q'q}f_{q'}(\mathbf{r}), \tag{37}$$

with $\langle g_q|g_{q'}\rangle=\delta_{qq'}$. Our strategy is to use the orbitals g_q as a new basis and discard the functions that correspond to $\sigma_q<\epsilon$ (we used $\epsilon=10^{-6}$). This leads to a much reduced basis as compared to the set of all functions f_q. As described in Ref. 52, this corresponds to discarding functions that are nearly linearly dependent and contribute little in the expansion.

The quantities Σ, $\tilde{W}$, and P will be represented in this new basis using

$$f_q(\mathbf{r})=\sum_{q'} g_{q'}(\mathbf{r})\sqrt{\sigma_{q'}}U^\dagger_{q'q}. \tag{38}$$

For the irreducible polarization we then find from Eq. (32) that

$$\begin{aligned}P(\mathbf{r}_1,\mathbf{r}_2;\tau)&=\sum_{qq'} P_{qq'}(\tau)f_q(\mathbf{r}_1)f^*_{q'}(\mathbf{r}_2)\\&=\sum_{q_1q_2}\left[\sum_{qq'} U^\dagger_{q_1q}P_{qq'}(\tau)U_{q'q_2}\right]\sqrt{\sigma_{q_1}\sigma_{q_2}}g_{q_1}(\mathbf{r}_1)\\&\quad\times g^*_{q_2}(\mathbf{r}_2),\end{aligned} \tag{39}$$

where

$$P_{qq'}(\tau)=2G_{ij}(\tau)G_{kl}(-\tau). \tag{40}$$

With $q=(il)$ and $q'=(jk)$ we have

$$P(\mathbf{r}_1,\mathbf{r}_2;\tau)=\sum_{q_1q_2}\tilde{P}_{q_1q_2}g_{q_1}(\mathbf{r}_1)g^*_{q_2}(\mathbf{r}_2), \tag{41}$$

where

$$\tilde{P}_{q_1q_2}=[\sqrt{\sigma}U^\dagger P(\tau)U\sqrt{\sigma}]_{q_1q_2}, \tag{42}$$

and $\sqrt{\sigma}$ is the diagonal matrix $(\sqrt{\sigma})_{pq}=\delta_{pq}\sqrt{\sigma_q}$. To calculate the screened potential we now insert Eq. (41) into Eq. (30) and readily obtain the matrix product

$$\tilde{W}_{qq'}(\tau)=[v\tilde{P}(\tau)v]_{qq'}+[v\tilde{P}(\tau-\tau')\tilde{W}(\tau')]_{qq'}, \tag{43}$$

where we defined the matrices

$$\tilde{W}_{qq'}=\int d^3\mathbf{r}_1d^3\mathbf{r}_2g^*_q(\mathbf{r}_1)\tilde{W}(\mathbf{r}_1,\mathbf{r}_2;\tau),g_{q'}(\mathbf{r}_2), \tag{44}$$

and

$$v_{qq'}=\int d^3\mathbf{r}_1d^3\mathbf{r}_2g^*_q(\mathbf{r}_1)v(\mathbf{r}_1,\mathbf{r}_2)g_{q'}(\mathbf{r}_2). \tag{45}$$

It is important to note that in Eqs. (41) and (43) the summation only runs over the indices q for which $\sigma_q>\epsilon$. We see from Eq. (42) that terms with $\sigma_q<\epsilon$ contribute little to the total sum. This leads to a considerable reduction in the number of matrix elements for v, P, and $\tilde{W}$. Finally the correlation part of the self-energy of Eq. (29) is given by

$$\begin{aligned}\Sigma_{r,ij}(\tau)&=\int d^3\mathbf{r}_1\int d^3\mathbf{r}_2\phi^*_i(\mathbf{r}_1)\Sigma_c(\mathbf{r}_1,\mathbf{r}_2;\tau)\phi_j(\mathbf{r}_2)\\&=-\sum_{kl}G_{kl}(\tau)\sum_{pq}\tilde{W}_{pq}(\tau)\int d^3\mathbf{r}_1\phi^*_i(\mathbf{r}_1)\phi_k(\mathbf{r}_1)\\&\quad\times g_p(\mathbf{r}_1)\int d^3\mathbf{r}_2\phi_j(\mathbf{r}_2)\phi^*_l(\mathbf{r}_2)g^*_q(\mathbf{r}_2)\\&=-\sum_{kl}G_{kl}(\tau)Z_{ik,jl},\end{aligned} \tag{46}$$

where

$$Z_{ik,jl}=\sum_{pq}\sqrt{\sigma_p}U_{ik,p}\tilde{W}_{pq}(\tau)U^\dagger_{q,jl}\sqrt{\sigma_q}. \tag{47}$$

We can summarize our procedure as follows: In the first step the overlap matrix $S_{qq'}$ of Eq. (35) is obtained and diagonalized. Further, using and Eqs. (37) and (45) the two-electron integrals in the new basis v_{pq} are constructed for p and q such that σ_p, $\sigma_q>\epsilon$. Subsequently, for the same values of p and q the matrix $\tilde{P}_{pq}(\tau)$ is constructed from Eq. (42) and $\tilde{W}_{pq}(\tau)$ is solved from Eq. (43). In the last step, the matrix (47) is obtained and the self-energy is calculated from Eq. (46) and further used in the solution of the Dyson equation.

V. RESULTS

The various GW schemes described in Sec. III are applied to a set of atoms and diatomic molecules using the computational method of Sec. IV. Details on the basis sets are provided in Ref. 53. In general we found that in single processor calculations, the computational cost of the GW_{fc} method is comparable to that of the G_0W_0 method and roughly twice as fast as the GW_0 method. The fully SCGW calculations were the most time consuming.

A. Particle number conservation

We start by investigating the number conservation property of the different GW schemes. In Fig. 2 we display the particle number obtained from the trace of the Green function for the case of the hydrogen molecule H_2 for different separations of the nuclei. We display results for the case of

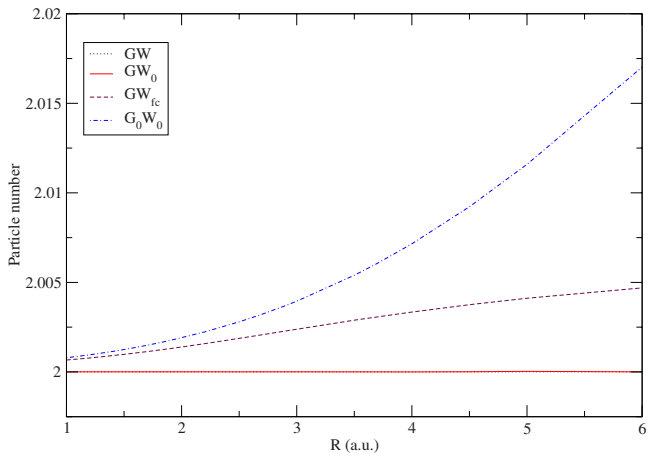

FIG. 2. (Color online) Particle number for H_2 at different interatomic distances within the SC-GW, GW_0, GW_{fc}, and G_0W_0 approximations.

SC-GW, GW_0, GW_{fc}, and G_0W_0, in which the reference Green function G_0 is obtained from a HF calculation. We see that the SC-GW and GW_0 schemes yield an integer particle number of $N=2$ for all internuclear separations. This is a consequence of the number conserving property of both approximations. This can be seen as follows. If we would adiabatically switch on the two-particle interactions from zero to full coupling strength within a conserving scheme, then the particle number would be conserved during the switching. This is because the conserving property is independent of the strength of the interaction and follows from the structure of the Φ functional only. Therefore the particle number of the final correlated state will be the same as the particle number of the initially noninteracting system. Hence conserving schemes always yield integer particle number for finite systems at zero temperature. For the case of the hydrogen molecule this is $N=2$ for all bond distances. For the case of G_0W_0 we see that the particle number conservation is violated as the particle number deviates from $N=2$ for all bond distances, the largest deviations occurring for the larger bond distances. For the larger separations, left-right correlation[54] in the hydrogen molecule, not incorporated in the HF part of the self-energy, becomes increasingly important. This puts more demands on the quality of the correlation part of the self-energy and consequently nonconservation of the particle number becomes more apparent at longer bond distances. Although the violation seems small (about 0.01 electron at $R=4.5$) it should be emphasized that a change in particle number of 0.05 can give large changes in the spectral features and conductive properties for molecules attached to leads. A clear example of this is presented in the work of Thygesen.[16] For the GW_{fc} (see Sec. III C) we also observe a violation of the number conservation law with increasing error for larger internuclear separations. The error with respect to G_0W_0 is, however, reduced by a factor of 3 at $R=5.5$ as a consequence of a partial inclusion of self-consistency.

B. Ground state energies

For the various GW schemes of Sec. III we calculated the total energies of some atoms and diatomic molecules from Eq. (11). The reference Green function G_0 for the non-self-consistent schemes was obtained from a HF calculation. In Table I we show the results. From comparison with benchmark configuration interaction (CI) results we see that the total energies of atoms and molecules calculated within all schemes are not very accurate. However, as we will see later, energy differences are much better produced. We can nevertheless make a number of useful observations from the total energies. We first note that all approximations produce a total energy that is lower than the benchmark CI result, with the G_0W_0 generally producing the lowest and thereby the worst values. Both the GW_0 and the GW_{fc} methods yield total energies in excellent agreement with SC-GW results, where for most systems the difference is 10^{-3} hartrees or less. This means that both the GW_0 and the GW_{fc} methods can be used to make an accurate prediction for the SC-GW energy at a much lower computational cost than the fully self-consistent calculation.

C. Binding curve

The calculation of binding curves is a good test for the quality of total energy calculations. In Fig. 3 we display the binding curve of the H_2 molecule for the various GW schemes together with benchmark CI results. The reference Green function G_0 was taken from a HF calculation. We further checked that using a G_0 obtained from a local density approximation LDA calculation only influences the results

TABLE I. Total energies (in hartrees) calculated from the GWA at various levels of self-consistency compared to CI values.

System	$E^{G_0W_0}[G_{HF}]$	$E^{GW_0}[G_{HF}]$	$E^{GW_{fc}}[G_{HF}]$	E_{SC}^{GW}	CI
He	−2.9354	−2.9271	−2.9277	−2.9278	−2.9037[a]
Be	−14.7405	−14.6882	−14.7032	−14.7024	−14.6674[a]
Be^{2+}	−13.6929	−13.6886	−13.6887	−13.6885	−13.6556[a]
Ne	−129.0885	−129.0517	−129.0506	−129.0499	−128.9376[a]
Mg	−200.2924	−200.1759	−200.1775	−200.1762	−200.053[a]
Mg^{2+}	−199.3785	−199.3451	−199.3454	−199.3457	−199.2204[a]
H_2	−1.1985	−1.1889	−1.1891	−1.1887	−1.133[b]
LiH	−8.1113	−8.0999	−8.0997	−8.0995	−8.040[c]

[a]From Ref. 55.
[b]From Ref. 56.
[c]From Ref. 57.

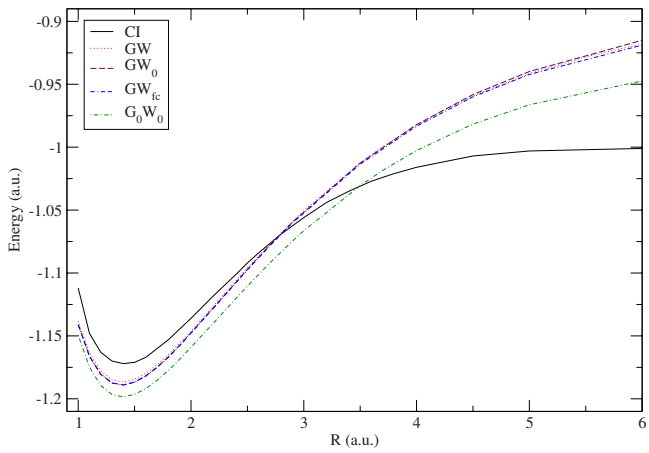

FIG. 3. (Color online) The total energy of the H_2 molecule as a function of the interatomic distance calculated from the GWA at various levels of self-consistency and CI (Ref. 56).

slightly. For the values of the energies around the bond minimum we see the same trend that we observed before: all GW schemes lead to a total energy that is lower than the benchmark CI results with G_0W_0 being the lowest. The total energies of the partially self-consistent schemes GW_0 and GW_{fc} are very close to the fully SCGW results for all bond distances. Although all GW schemes considerably improve the bonding curve obtained from an uncorrelated HF calculation, it is clear that all these schemes deviate considerably from the CI results in the infinite atomic separation limit. To cure this feature one either has to do a spin-polarized calculation or go beyond the GWA and include vertex diagrams in the diagrammatic expansion for the self-energy. The shape of the binding curve around the bond minimum is well reproduced by the SC-GW, GW_0, and GW_{fc} schemes, implying that these methods may be used to obtain accurate vibrational frequencies. Since the shape of the bonding curve is only determined by total energy differences, this already indicates that these approximations may perform better in obtaining the energy differences than in obtaining total energies.

D. Two-electron removal energies

To test the performance of the various GW schemes in obtaining energy differences, we investigated the two-electron removal energies of the beryllium and magnesium atom. Since these atoms and their doubly ionized counterparts are closed shell they were suitable test systems. Moreover, the beryllium atom is a well-known case for which electron correlations play an important role due to strong mixing of the $2s$ and $2p$ states in a configuration expansion. In Table II, we display the two-electron removal energies for various GW schemes as well as for the HF approximation. The reference Green function G_0 is again obtained from a HF calculation. The self-consistent and partially SCGW schemes yield results within 0.1 eV from the experimental values and considerably improve the HF values that differ with more than 1 eV from experiment. The G_0W_0 approximation does not improve at all on the HF approximation and gives considerably worse results than the other GW schemes. We further see that both the GW_0 and the GW_{fc} approximations give removal energies that are in excellent agreement with the fully SCGW results.

E. Ionization potentials

In Table III we show the ionization potentials obtained with the various GW methods for a number of atoms and diatomic molecules. These ionization potentials were obtained using the extended Koopmans theorem, as explained in Appendix A. For G_0W_0 the results shown in the first column were obtained by using a reference Green function G_0 from a local density functional (LDA) calculation using the parametrization of the exchange-correlation functional due to Vosko *et al.*[59] In all other cases we used a reference Green function from a HF calculation. We see that the ionization potentials of fully SCGW agree well with the experimental values, the main exceptions being the H_2 molecule and the Be atom, which show a deviation of, respectively, 0.8 and 0.5 eV. The other partially self-consistent approaches GW_0 and GW_{fc} yield results that are very close to the fully self-consistent results. The G_0W_0 approximation based on the LDA reference Green function performs a bit worse than the SCGW scheme. For He and LiH there is an error of about 1 eV and for Ne and for H_2 an error of about 0.5 eV. Performing a G_0W_0 calculation based on a HF reference G_0 instead improves the results for several systems but worsens the agreement for H_2 which is 1.1 eV in error. The dependence on the reference Green function G_0 within the G_0W_0 method is clearly unsatisfactory. The partially self-consistent approximations suffer much less from this problem. For those schemes we found that changing the reference Green function from a HF one to a LDA one only slightly changes the results.

VI. SUMMARY AND CONCLUSIONS

We investigated the performance of the GW at different levels of self-consistency for the cases of atoms and diatomic molecules. Our main motivation for studying fully self-consistent Φ-derivable schemes was that they provide unambiguous results for different observables and the fact that they satisfy important conservation laws that are important in future nonequilibrium applications of the theory.[18] We adressed the question to what extent partially self-consistent

TABLE II. Two-electron removal energies $E_{N-2}-E_N$ (in eV) calculated from the HF and from the GWA at various levels of self-consistency compared to the experimental values.

System	HF	$\Delta E^{G_0W_0}$	ΔE^{GW_0}	$\Delta E^{GW_{fc}}$	ΔE_{SC}^{GW}	Exp.[a]
$Mg-Mg^{2+}$	21.33	24.86	22.61	22.64	22.59	22.68
$Be-Be^{2+}$	26.17	28.50	27.20	27.61	27.59	27.53

[a]From Ref. 58.

TABLE III. Ionization potentials (eV) calculated from the extended Koopmans theorem from various *GW* approaches.

System	$G_0^{(\mathrm{LDA})}W_0$	$G_0^{(\mathrm{HF})}G_{W_0}$	GW_0	GW_{fc}	SC-*GW*	Exp.[a]
He	23.65	24.75	24.59	24.56	24.56	24.59
Be	8.88	9.19	8.82	8.81	8.66	9.32
Ne	21.06	21.91	21.90	21.82	21.77	21.56
Mg	7.52	7.69	7.43	7.38	7.28	7.65
H_2	15.92	16.52	16.31	16.22	16.22	15.43
LiH	6.87	8.19	7.71	7.85	7.85	7.9

[a]From Ref. 58.

schemes can reproduce the results of a fully SCGW calculation. We found that both the GW_0 method as well as the GW_{fc} scheme proposed by us yield results in close agreement with fully SCGW calculations. We further checked the number conservation properties of the various schemes. The fully SCGW scheme being Φ-derivable does satisfy all conservation laws, but also the partially self-consistent GW_0 approximation was shown to be number conserving. The non-self-consistent G_0W_0 and the partially self-consistent GW_{fc} approximations both violate the number conservation laws but due to the partial self-consistency in GW_{fc}, the errors are much reduced in this scheme. A major advantage of the latter scheme is, however, that it produces results that are close to the fully SCGW results at a much lower computational cost. It will therefore be very valuable to test this method on solid state systems for which SCGW calculations are difficult to perform due to the large computational effort. In this way it will be possible to get further insight into the performance of SCGW for a large class of extended systems. Work on application of the fully SCGW method to transport phenomena is in progress.[18]

APPENDIX A: IONIZATION POTENTIALS FROM THE EXTENDED KOOPMANS THEOREM

Here we give a brief description on the way we extract the ionization energies from the Green function using the extended Koopmans theorem.[41–45] As input, this method only needs the Green function and its time derivative at $\tau=0^-$ on the imaginary time axis. We define an $N-1$ particle state

$$|\Phi^{N-1}[u_i]\rangle = \int d\mathbf{x} u_i(\mathbf{x})\hat{\psi}(\mathbf{x})|\Psi_0^N\rangle, \tag{A1}$$

where $u_i(\mathbf{x})$ is determined by requiring the functional

$$E^{N-1}[u_i] = \frac{\langle\Phi^{N-1}[u_i]|\hat{H}|\Phi^{N-1}[u_i]\rangle}{\langle\Phi_{N-1}[u_i]|\Phi_{N-1}[u_i]\rangle}, \tag{A2}$$

which describes the energy of the $N-1$ particle system, to be stationary with respect to variations in u_i. This amounts to minimizing the energy of the $N-1$ system by choosing an optimal value for u_i. We find

$$\int d\mathbf{x}\langle\Psi_0^N|\hat{\psi}^\dagger(\mathbf{x}')[\hat{\psi}(\mathbf{x}),\hat{H}]|\Psi_0^N\rangle u_i(\mathbf{x}) = (E_0^N - E_i^{N-1})\int d\mathbf{x}\langle\Psi_0^N|\hat{\psi}^\dagger(\mathbf{x}')\hat{\psi}(\mathbf{x})|\Psi_0^N\rangle u_i(\mathbf{x}), \tag{A3}$$

where the last term contains the density matrix. This quantity is easily obtained from the Green function as

$$\rho(\mathbf{x},\mathbf{x}') = \langle\psi_0^N|\hat{\psi}_H^\dagger(\mathbf{x}'\tau)\hat{\psi}_H(\mathbf{x}\tau)|\Psi_0^N\rangle = \lim_{\eta\to 0} G(\mathbf{x},\mathbf{x}',-\eta), \tag{A4}$$

i.e., $\rho(\mathbf{x},\mathbf{x}')=\tilde{G}(\mathbf{x},\mathbf{x}';0^-)$ or $\rho_{ij}=G_{ij}(0^-)$ in molecular orbital basis.[40] Also the expectation value under the integral on the right hand side of Eq. (A3) is easily obtained from the Green function,

$$-\partial_\tau G(\mathbf{x},\mathbf{x}';\tau)|_{\tau=0^-} = \langle\psi_0^N|\hat{\psi}^\dagger(\mathbf{x}')[\hat{\psi}(\mathbf{x}),\hat{H}]|\Psi_0^N\rangle = \Delta(\mathbf{x},\mathbf{x}'). \tag{A5}$$

In this derivation we used a zero-temperature formulation but making a connection to the finite temperature formalism is straightforward. When we take into account that in the finite temperature formalism we included the chemical potential in the one-body part of the Hamiltonian [see Eq. (2)], then from Eqs. (A3) and (A5) we obtain the eigenvalue equation

$$\int d\mathbf{x}\Delta(\mathbf{x},\mathbf{x}')u_i(\mathbf{x}) = (E_0^N - E_i^{N-1} - \mu)\int d\mathbf{x}\rho(\mathbf{x},\mathbf{x}')u_i(\mathbf{x}), \tag{A6}$$

where ρ and Δ are calculated according to Eqs. (A4) and (A5). A similar equation for the electron affinities can similarly be derived starting from an $N+1$ state. Since both matrices ρ and Δ are easily evaluated from the Green function, Eq. (A6) provides an easy way to extract removal energies from knowledge of the Green function on the imaginary time axis.

For completeness we mention that the extended Koopmans method also provides a simple way to extract quasiparticle or Dyson orbitals[45] and to construct the Green function on the real frequency axis. The Dyson orbitals are given by

$$f_i(\mathbf{x}) = \langle \Phi_i^{N-1} | \hat{\psi}(\mathbf{x}) | \Psi_0^N \rangle$$
$$= \int d\mathbf{x}' u_i^*(\mathbf{x}') \langle \Psi^N | \hat{\psi}^\dagger(\mathbf{x}') \hat{\psi}(\mathbf{x}) | \Psi_0^N \rangle$$
$$= \int d\mathbf{x}' \rho(\mathbf{x},\mathbf{x}') u_i^*(\mathbf{x}'). \tag{A7}$$

In terms of these orbitals and the extended Koopmans eigenvalues the hole part of the Green function is then given on the real frequency axis as

$$G(\mathbf{x},\mathbf{x}';\omega) = \sum_n \frac{f_n(\mathbf{x}) f_n^*(\mathbf{x}')}{\omega - (E_0^N - E_n^{N-1} + \mu) + i\eta}.$$

Similar derivations can be carried out for the affinities and the corresponding Dyson orbitals from which the particle part of the Green function can be constructed on the real axis.

APPENDIX B: THE UNIFORM POWER MESH

The UPM (Ref. 20) is a one-dimensional grid on an interval $[0,\beta]$ which becomes more dense at the endpoints. Therefore, it is well suited to describe the Green function on the imaginary time axis, since it behaves exponentially around $\tau=0$ and $\tau=\pm\beta$,[20,40] The UPM is defined by two integers u and p and the length of the interval β. The procedure to construct it is simple: we consider the $2(p-1)$ intervals $[0,\beta_j]$ and $[\beta-\beta_j,\beta]$ for $j=1,\ldots,p-1$ with $\beta_j=\beta/2^j$ and divide each of these intervals in $2u$ subintervals of equal length. The endpoints of all these intervals define our grid which has $2pu+1$ grid points.

[1] A. L. Fetter and J. D. Walecka, *Quantum Theory of Many-Particle Systems* (McGraw-Hill, New York, 1971).
[2] E. K. U. Gross, E. Runge, and O. Heinonen, *Many-Particle Theory* (Hilger, Bristol, 1991).
[3] F. Aryasetiawan and O. Gunnarsson, Rep. Prog. Phys. **61**, 237 (1998).
[4] W. Aulbur, L. Jönsson, and J. Wilkins, Solid State Phys. **54**, 1 (2000).
[5] L. Hedin, Phys. Rev. **139**, A796 (1965).
[6] R. M. Dreizler and E. K. U. Gross, *Density Functional Theory, An Approach to the Quantum Many-Body Problem* (Springer-Verlag, Berlin, 1990).
[7] G. D. Mahan, Comments Condens. Matter Phys. **16**, 333 (1994).
[8] B. Holm and U. von Barth, Phys. Rev. B **57**, 2108 (1998).
[9] T. J. Pollehn, A. Schindlmayr, and R. W. Godby, J. Phys.: Condens. Matter **10**, 1273 (1998).
[10] G. Baym, Phys. Rev. **127**, 1391 (1962).
[11] G. Baym and L. P. Kadanoff, Phys. Rev. **124**, 287 (1961).
[12] M. Bonitz, K. Balzer, and R. van Leeuwen, Phys. Rev. B **76**, 045341 (2007).
[13] C.-O. Almbladh, U. Barth, and R. Leeuwen, Int. J. Mod. Phys. B **13**, 535 (1999).
[14] K. S. Thygesen and A. Rubio, Phys. Rev. B **77**, 115333 (2008).
[15] K. S. Thygesen and A. Rubio, J. Chem. Phys. **126**, 091101 (2007).
[16] K. S. Thygesen, Phys. Rev. Lett. **100**, 166804 (2008).
[17] X. Wang, C. D. Spataru, M. S. Hybertsen, and A. J. Millis, Phys. Rev. B **77**, 045119 (2008).
[18] P. Myöhanen, A. Stan, G. Stefanucci, and R. van Leeuwen, Europhys. Lett. **84**, 67001 (2008).
[19] A. Schindlmayr and R. W. Godby, Phys. Rev. Lett. **80**, 1702 (1998).
[20] W. Ku and A. G. Eguiluz, Phys. Rev. Lett. **89**, 126401 (2002).
[21] K. Delaney, P. García-González, A. Rubio, P. Rinke, and R. W. Godby, Phys. Rev. Lett. **93**, 249701 (2004).
[22] B. Holm, Phys. Rev. Lett. **83**, 788 (1999).
[23] P. García-González and R. W. Godby, Phys. Rev. B **63**, 075112 (2001).
[24] B. Holm and U. von Barth, Phys. Scr., T **T109**, 135 (2004).
[25] V. M. Galitskii and A. B. Migdal, Zh. Eksp. Teor. Fiz. **34**, 139 (1958); [Sov. Phys. JETP **7**, 96 (1958)].
[26] N. E. Dahlen, R. van Leeuwen, and U. von Barth, Phys. Rev. A **73**, 012511 (2006).
[27] R. van Leeuwen, N. E. Dahlen, and A. Stan, Phys. Rev. B **74**, 195105 (2006).
[28] M. P. Agnihotri, W. Apel, and W. Weller, Phys. Status Solidi B **245**, 421 (2008).
[29] U. von Barth and B. Holm, Phys. Rev. B **54**, 8411 (1996).
[30] T. Kotani and M. van Schilfgaarde, Solid State Commun. **121**, 461 (2002).
[31] S. V. Faleev, M. van Schilfgaarde, and T. Kotani, Phys. Rev. Lett. **93**, 126406 (2004).
[32] M. van Schilfgaarde, T. Kotani, and S. Faleev, Phys. Rev. Lett. **96**, 226402 (2006).
[33] S. V. Faleev, M. van Schilfgaarde, T. Kotani, F. Léonard, and M. P. Desjarlais, Phys. Rev. B **74**, 033101 (2006).
[34] F. Bruneval, N. Vast, and L. Reining, Phys. Rev. B **74**, 045102 (2006).
[35] A. Stan, N. E. Dahlen, and R. van Leeuwen, Europhys. Lett. **76**, 298 (2006).
[36] T. Matsubara, Prog. Theor. Phys. **14**, 351 (1955).
[37] L. V. Keldysh, Zh. Eksp. Teor. Fiz. **47**, 1515 (1964); [Sov. Phys. JETP **20**, 1018 (1965)].
[38] P. Danielewicz, Ann. Phys. (N.Y.) **152**, 239 (1984).
[39] M. Wagner, Phys. Rev. B **44**, 6104 (1996).
[40] N. E. Dahlen and R. van Leeuwen, J. Chem. Phys. **122**, 164102 (2005).
[41] J. Katriel and E. R. Davidson, Proc. Natl. Acad. Sci. U.S.A. **77**, 4403 (1980).
[42] O. W. Day, D. W. Smith, and R. C. Morrison, J. Chem. Phys. **62**, 115 (1975).
[43] D. W. Smith and O. W. Day, J. Chem. Phys. **62**, 113 (1975).
[44] D. Sundholm and J. Olsen, J. Chem. Phys. **98**, 3999 (1993).
[45] R. C. Morrison and P. W. Ayers, J. Chem. Phys. **103**, 6556 (1995).
[46] L. Hedin, A. Johansson, B. I. Lundqvist, S. Lundqvist, and V. Samathiyakanit, Ark. Fys. **39**, 97 (1968).
[47] H. N. Rojas, R. W. Godby, and R. J. Needs, Phys. Rev. Lett. **74**, 1827 (1995).
[48] C. Fortmann, Trends Stat. Phys. **41**, 445501 (2008).
[49] B. Holm, Ph.D. thesis, Lund University, 1997.
[50] N. H. Hugenholtz and L. van Hove, Physica (Amsterdam) **24**, 363 (1958).
[51] N. E. Dahlen, A. Stan, and R. van Leeuwen, J. Phys.: Conf. Ser. **35**, 324 (2006).
[52] F. Aryasetiawan and O. Gunnarsson, Phys. Rev. B **49**, 16214 (1994).
[53] See EPAPS Document No. E-JCPSA6-130-036910 for basis sets. For more information on EPAPS, see http://www.aip.org/pubservs/epaps.html.
[54] E. J. Baerends and O. V. Gritsenko, J. Phys. Chem. A **101**, 5383 (1997).
[55] S. J. Chakravorty, S. R. Gwaltney, E. R. Davidson, F. A. Parpia, and C. F. Fischer, Phys. Rev. A **47**, 3649 (1993).
[56] R. van Leeuwen, Ph.D. thesis, Vrije Universiteit, 1994.
[57] X. Li and J. Paldus, J. Chem. Phys. **118**, 2470 (2003).
[58] S. G. Lias, R. D. Levin, and S. A. Kafafi, Ion Energetics Data in NIST Chemistry Web-Book, NIST Standard Reference Database Number 69, edited by P. J. Linstrom and W. G. Mallard, March 2003, National Institute of Standards and Technology, Gaithersburg, MD, 20899 (http://webbook.nist.gov).
[59] S. H. Vosko, L. Wilk, and M. Nusair, Can. J. Phys. **58**, 1200 (1980).